Pergamon

Cement and Concrete Research 30 (2000) 849–854

CEMENT AND CONCRETE RESEARCH

Automated identification of the aggregate–paste interfacial transition zone in mortars of silica sand with Portland or alkali-activated slag cement paste

A.R. Brough*, A. Atkinson

Department of Materials, Imperial College, Prince Consort Road, London SW7 2BP UK

Received 1 February 1999; accepted 2 March 2000

Abstract

The interfacial transition zone (ITZ) between cement paste and aggregate strongly influences the mechanical and transport properties of mortar and concrete. Backscattered electron (BSE) imaging in the scanning electron allows anhydrous cement, hydration products, and porosity in this region to be quantified by compositional contrast. When the aggregate has a similar brightness to the hydrates, as in some alkali-activated cement mortars with silica sand, automated identification of the aggregate edge in the BSE image is difficult. Manual identification is laborious and prone to errors. Here we demonstrate use of energy dispersive X-ray (EDX) dot maps, acquired concurrently with the BSE to enable *compositional* identification of the aggregate edge automatically. The mortars studied were prepared with OPC or slag activated with either sodium silicate or potassium hydroxide. The edges of the silica sand aggregate particles were located to within 2.5 μm, and the gradation of microstructure across the ITZ was quantified automatically. Hydrates were found most successfully to infill the ITZ in sodium silicate-activated slag cement mortars.

Keywords: Interfacial transition zone; Image analysis; Backscattered electron imaging; SEM; Alkali-activated slag

1. Introduction

The interfacial zone between bulk paste and aggregate surfaces is important, since the enhanced porosity in this region may lead to a percolating path into the cement paste [1], and thus to reduced durability. Studies of the interfacial zone were reviewed in 1995 [2]. This zone has been characterized by image analysis of backscattered electron (BSE) images from polished sections in the electron microscope, once the aggregate particles have been identified. Sometimes this identification is simple, as when cement paste is cast against a flat, polished aggregate surface, but in real systems, it can be more difficult. For example, Crumbie [3] has identified aggregate manually by digitization of a series of points defining the boundary of each aggregate particle; in addition to being extremely laborious, this method is prone to systematic and random errors, especially given that for most applications, many images must be processed in order to achieve statistically significant results. In alkali-activated slag systems with silica aggregate, the hydrate gel often has a similar backscattered coefficient to the silica aggregate, making identification of the aggregate and paste more difficult.

In this article, we describe one possible way in which aggregate particles can be identified automatically on the basis of composition. Such use of compositional data has been reported previously, as for example in the identification of the various phases in cement clinker [4], or in the visual identification of the aggregate paste interface [5]. Our work here differs in that we aim to acquire the compositional data in tandem with the BSE image that will be used to distinguish between anhydrous cement and hydration products, and on the same time scale as would usually be used to acquire this image. We demonstrate the technique for silica sand mortars with OPC paste and with waterglass and potassium hydroxide activated alkali-activated slag pastes. In each case, we analyze the properties of the bulk paste and of the interfacial zone.

* Corresponding author. Departments of Civil Engineering and Materials, University of Leeds, Leeds, LS2 9JT, UK. Tel.: +44-113-233-2306; fax: +44-113-233-2265.

E-mail address: a.r.brough@leeds.ac.uk (A.R. Brough).

0008-8846/00/$ – see front matter
PII: S0008-8846(00)00254-4

Table 1
Particle size distributions for the slag and OPC

Size/μm	Slag	OPC
>40	8	17
20–40	23	24
10–20	22	17
<10	47	42

2. Experimental

Particle size distributions for the cement and slag are given in Table 1. Mortar specimens were prepared using the 300–600 μm fraction sieved from a Class M silica sand. Mix proportions of 0.5 ml solution / 1 g binder / 2.33 g air-dried aggregate were used. The solids were premixed for 1 min, and then the solution added, and the mortar mixed for a further 2 min at slow speed in a planetary mixer. The bowl was then scraped down, and the mortar mixed for a further 1 min at fast speed and 1 min at slow speed. The samples were cast into sealed plastic tubes and cured in a humidistat at 20°C and > 95% relative humidity. Samples for microscopy were sectioned so the fields of view had been horizontal during setting, and were then freeze-dried and stabilized by vacuum impregnation with a low viscosity epoxy resin. They were lapped flat with 9 μm Al_2O_3 suspended in ethylene glycol on a cast iron plate and polished successively with 9 μm silicon carbide paper, and with 3, 1, and 1/4 μm diamond paste. After the lapping stage, an additional epoxy impregnation was performed, if needed, and the samples were relapped, in order to ensure full resin impregnation and a good quality polish. The samples were then carbon-coated and BSE images and X-ray maps were acquired in a Jeol 35CF scanning electron microscope, equipped with a PGT IMIX-PTS EDS and image analysis system, and an Imix Prism Li drifted Si digital detector. Some resolution was lost in the microscope by using a long working distance in order to be able to obtain X-ray maps simultaneously with the BSE images, but this was not significant for the pixel size used for image acquisition. A probe current of approximately 2 nA was utilized, with the EDS crystal located at a distance of 40 mm (collimator somewhat closer than this) with a take-off angle of 35°, giving a count rate of approximately 6000 cps. Under these conditions, the spot size was less than 0.2 μm. The 512 * 512 pixel BSE images were acquired at a magnification of 400 × giving a resolution of 0.6 μm per pixel. (A larger probe current could have been used at this resolution, but generally resulted in some noticeable charging taking place.) The dot maps were acquired simultaneously at the lower resolution of 256 * 256 pixels, giving a resolution of 1.2 μm per pixel, which was adequate given the interfacial zone thickness of 20 μm. These parameters were chosen to enable the noise level in the X-ray map to be sufficiently low to identify the aggregate regions without

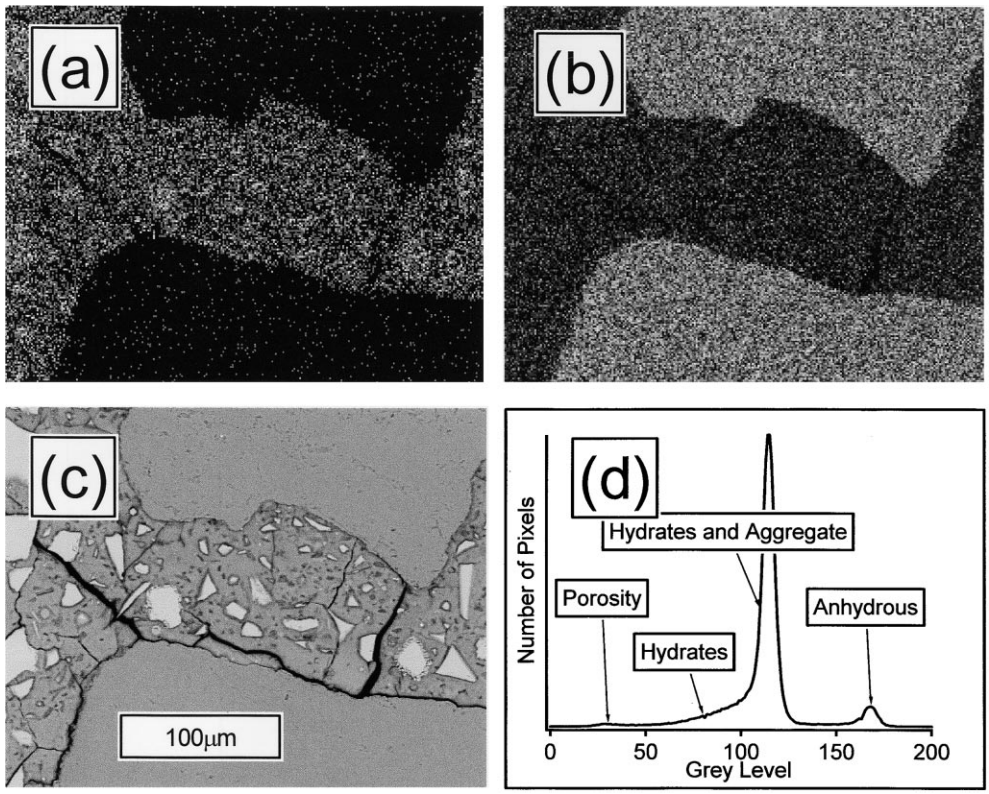

Fig. 1. Data as acquired. (a) Ca dot map, (b) Si dot map, (c) backscattered image, and (d) histogram for the backscattered image. (Grey level 0 is black, grey level 245 is white).

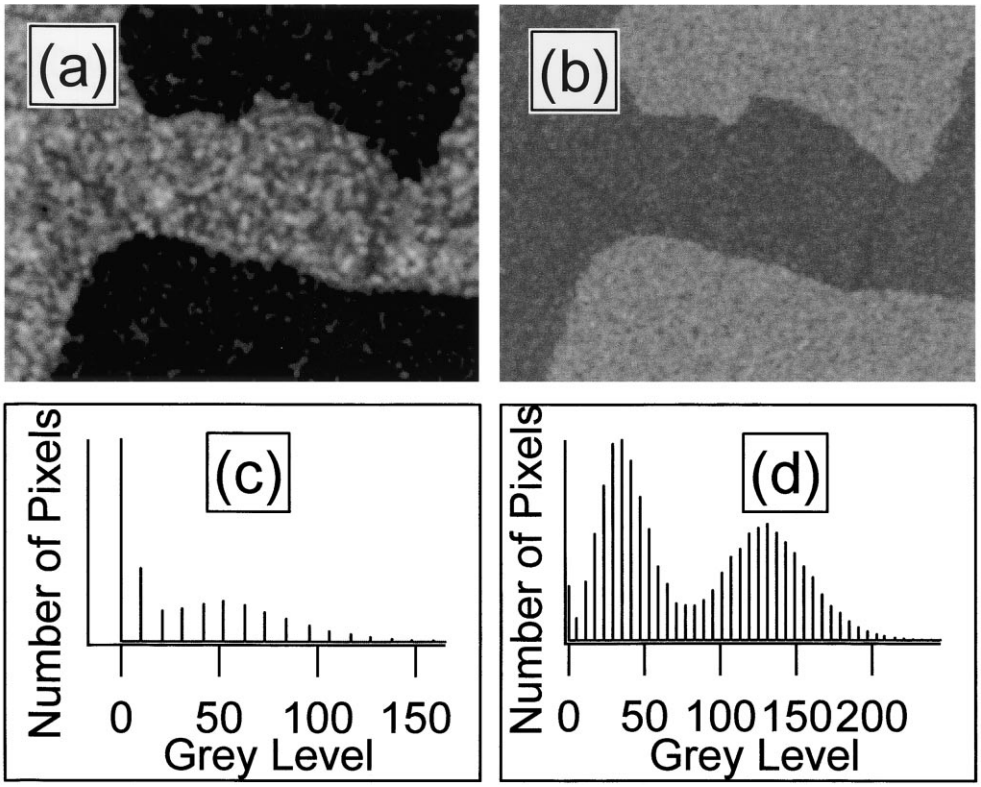

Fig. 2. Smoothed data. (a) Ca dot map, (b) Si dot map, (c) histogram for smoothed Ca dot map, and (d) histogram for smoothed Si dot map.

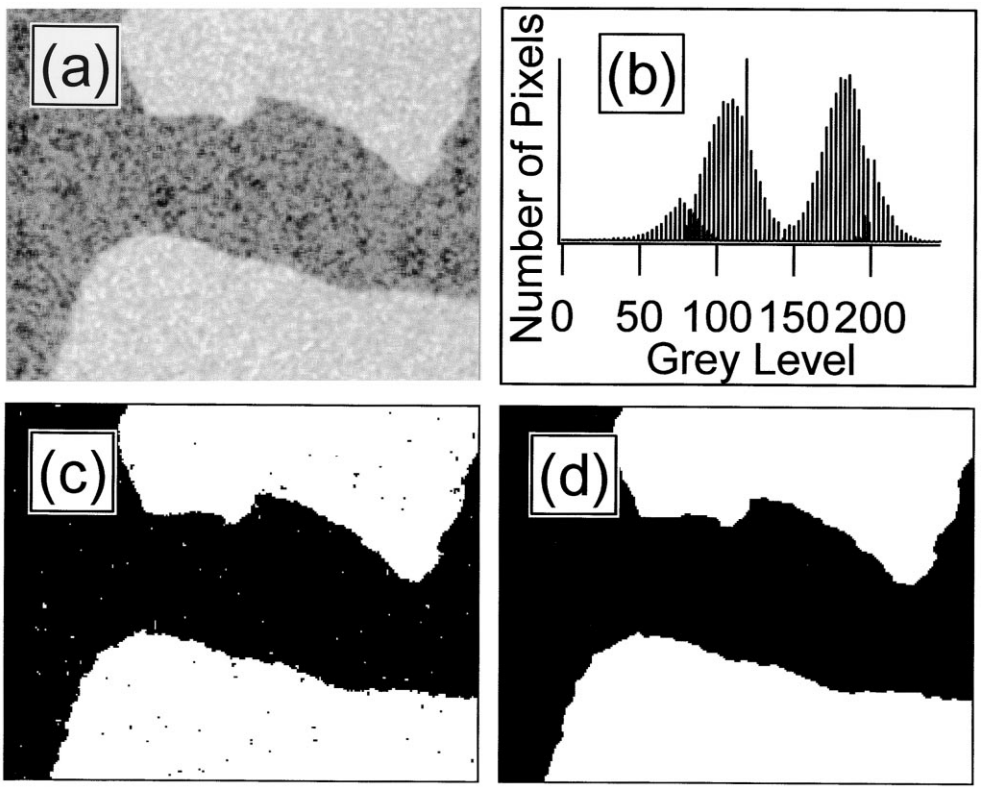

Fig. 3. (a) Composite image, Si−2*Ca, (b) histogram of (a), (c) segmented aggregate image, and (d) aggregate image after open/close operation.

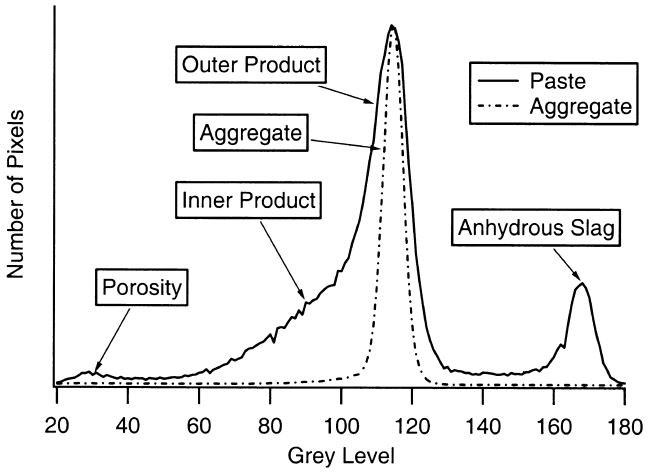

Fig. 4. Histogram of backscattered intensities for paste and aggregate areas of the BSE image.

necessitating a very long acquisition time. Data was averaged from five frames giving a total acquisition time of 180s per image including the EDS system dead time and movement of the stage between positions. Image locations were selected randomly and visually screened before acquisition to exclude any images which contained only aggregate, or in which there were significant polishing defects. Ca and Si dot maps were acquired and used to identify the aggregate locations. The aggregate image was used in combination with the BSE image for subsequent analysis of bulk or interfacial paste properties.

3. Results and discussion

Fig. 1 shows a typical set of images as acquired, with Ca and Si dot maps and a BSE image, along with a histogram for the BSE image; it can be seen from the BSE image and histogram that the hydrate gel and aggregate have similar backscattered coefficients. It is not possible to distinguish the aggregate directly from either dot map. There is no Ca in the aggregate, and yet there is also no Ca in some regions of the paste (outside anhydrous grains) at an early age, nor in cracks. The highest levels of Si are found in the aggregates, but the counting statistics are not sufficiently good to distinguish this from levels in denser regions of the paste. Fig. 2(a) and (b) shows the images made by smoothing the dot maps (simple 3 × 3 matrix mean). Again, it is not possible to distinguish quantitatively paste and aggregate as can be seen from the histograms in Fig. 2(c) and (d). However, a composite image (Fig. 3(a)) more clearly separates the regions (and works for a wide range of paste compositions and for systems at early and late ages), giving a better resolved aggregate peak in the histogram (Fig. 3(b)) and enabling segmentation of the aggregate (Fig. 3(c)). Small polishing imperfections and the remaining small overlap of the peaks lead to a number of minor defects that are easily removed by an open and close operation to give the final aggregate image shown in Fig. 3(d). Inspection of the images indicates that the interface is located within about 2.5 μm (i.e. 2 pixels in the X-ray map), with most edges considerably closer than this—some miss match is expected, since the X-ray maps sample deeper into the specimen surface than the BSE images.

The BSE image can then be analyzed allowing for the areas that are aggregate and paste. Fig. 4 shows the histograms for the aggregate and non-aggregate areas of the backscattered image; it can be seen that the paste histogram contains a bright peak due to aggregate, and a dark peak due to porosity, but that the central C-S-H peak has two components, one due to outer product, with a similar backscattered coefficient to the aggregate, and one which is slightly darker and broader, due to inner product.

The areas of anhydrous material and porosity in the paste fraction of the three systems were measured after 28 or 56 days hydration, and Table 2 shows the proportion of phases and extent of hydration in the three cases. A full study of a range of alkali-activated slag systems is under review [6].

With the aggregate and paste identified, it was also possible to measure the distribution of anhydrous material and coarse porosity against the interface. (Porosity finer than the 0.6 μm pixel size will not be observed.) Data were summed for the full series of images taken for each sample (Fig. 5). There is an excess of porosity and a deficit of anhydrous material next to the interface in all the systems studied, as is expected from the literature. The data were fitted to exponentials to assess the interfacial region quantitatively. The silicate-activated slag mortar has the least coarse porosity, and the OPC mortar has the most, with the increase in porosity close to the interface also being smallest for the silicate-activated system. In all cases, the anhydrous material falls off close to the interface, leading to the increased porosity, but in the case of the alkali silicate-

Table 2
The calculations for standard deviation and standard error allow for the fact that the images contain varying amounts of paste. For number of images, the paste area indicates the integrated area of paste over the full number of images

Cement system	Number of images (paste area)	Area percentage of phase (Standard deviation) (Standard error)		
		Anhydrous	Porosity	Hydration products
AAS (WG)	21 (10)	22.7 (4.4) (1.4)	3.7 (2.1) (0.7)	73.6
AAS (KOH)	27 (12)	16.6 (5.7) (1.6)	6.7 (5.7) (1.6)	76.7
OPC	39 (20)	8.0 (4.6) (1.0)	5.5 (2.6) (0.6)	86.5

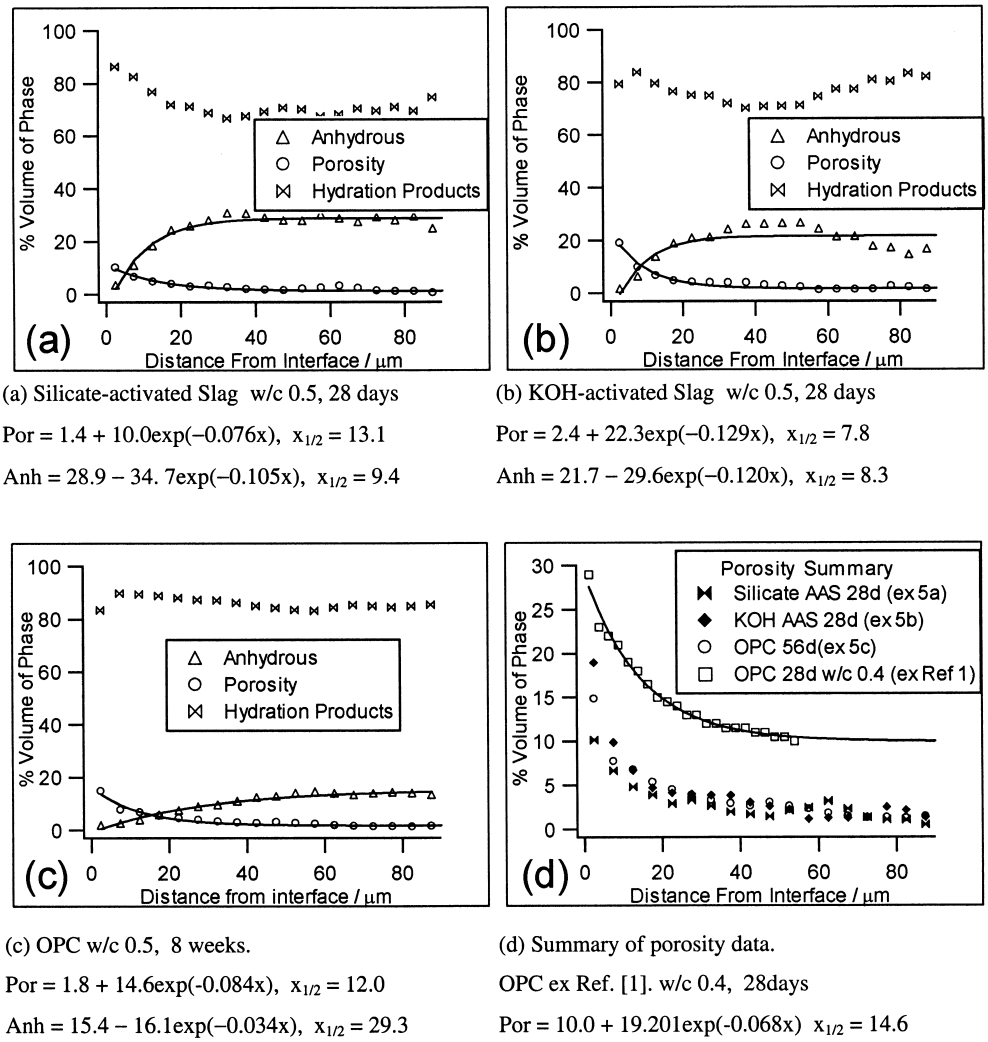

(a) Silicate-activated Slag w/c 0.5, 28 days

Por = 1.4 + 10.0exp(−0.076x), $x_{1/2}$ = 13.1

Anh = 28.9 − 34. 7exp(−0.105x), $x_{1/2}$ = 9.4

(b) KOH-activated Slag w/c 0.5, 28 days

Por = 2.4 + 22.3exp(−0.129x), $x_{1/2}$ = 7.8

Anh = 21.7 − 29.6exp(−0.120x), $x_{1/2}$ = 8.3

(c) OPC w/c 0.5, 8 weeks.

Por = 1.8 + 14.6exp(-0.084x), $x_{1/2}$ = 12.0

Anh = 15.4 − 16.1exp(−0.034x), $x_{1/2}$ = 29.3

(d) Summary of porosity data.

OPC ex Ref. [1]. w/c 0.4, 28days

Por = 10.0 + 19.201exp(-0.068x) $x_{1/2}$ = 14.6

Fig. 5. Distribution of hydration products relative to interface with aggregate; symbols indicate actual data, lines are curve fits, where x is the distance from the interface: (a) Waterglass-activated slag mortar, (b) KOH-activated slag mortar, (c) OPC mortar. Equations for the curve fits are given below the figures. (d) Summary of the porosity data, also showing data taken from Ref. [1] (OPC w/c 0.4, 28 days).

activated system, additional hydration products are found in this area, partially filling in the extra space in the microstructure. In fact, the filling in is almost complete, since it appears that most of the observed porosity is in fact shrinkage cracking arising from the sample preparation process. In all cases, the distribution of anhydrous materials against the interface fits fairly well to the exponential, with a decay length of approximately 9 μm for the slag systems, and 15 μm for the OPC, as expected for the slightly larger particle size distribution for the OPC.

4. Conclusions

Automated location of the aggregate was successful and within 2.5 μm of the edge as identified visually. The procedure was only slightly slower than acquisition of BSE images only, and led to much faster processing subsequently. Results obtained for the bulk properties of an OPC system were consistent with those reported previously in the literature, and the interfacial zone was also identified correctly. For KOH-activated slag mortar, similar results were obtained, while for sodium silicate-activated slag, there was no enhanced interfacial porosity, despite a lower extent of reaction. Even though the anhydrous material was still excluded from the region close to the aggregates at an early age, hydration products filled up this space in the system.

Acknowledgments

We thank EPSRC and the Cementitious Slag Makers Association for support under grant GR/K52201, the EPSRC for funding equipment under grant GR/L26537, and the Appleby Group and Crossfield for the supply of blast furnace slag and sodium silicates.

References

[1] K.L. Scrivener, K.M. Nemati, The percolation of pore space in the cement paste/aggregate interfacial zone of concrete, Cem Concr Res 26 (1996) 35–40.
[2] J.P. Ollivier, J.C. Maso, B. Bourdette, Interfacial transition zone in concrete, Adv Cem Based Mater 2 (1995) 30–38.
[3] A.K. Crumbie, Characterization of the microstructure of concrete, PhD Thesis, University of London, 1994.
[4] E. Backstrom, S. Hansen, X-ray mapping of interstitial phases in sulphate resisting cement clinker, Adv Cem Res 9 (1997) 17–23.
[5] M.H. Zhang, O.E. Gjorv, BSE imaging studies on the IFZ between high strength lightweight aggregate and cement paste, Adv Cem Res 2 (1989) 141–146.
[6] A.R. Brough, A. Atkinson, Sodium silicate based alkali activated slag mortars: Part I. Strength, hydration and microstructure, Cem Concr Res submitted for publication.